

# New dynamics in cerebellar Purkinje cells: limit cycle canards

Mark A. Kramer<sup>†</sup>, Roger D. Traub,<sup>\*</sup> and Nancy J. Kopell<sup>†</sup>

We describe a transition from bursting to rapid spiking in a reduced mathematical model of a cerebellar Purkinje cell. We examine the critical manifold of the slow-fast system and find that — after a saddle node bifurcation of limit cycles — the full model dynamics follow temporarily a repelling branch of limit cycles. We propose that the system exhibits a new type of dynamical phenomenon: limit cycle canards.

PACS numbers:

Bursting — a repeated pattern of alternating quiescence and rapid spiking — occurs in many neural systems, perhaps with functional implications [1, 2]. Mathematical models developed to characterize bursting neural activity typically share common dynamical traits (e.g., excitability, slow-fast dynamics) and bifurcations [3, 4]. In these models, the mechanisms that produce both periodic spiking and bursting activity are well understood [5, 6]. Yet the transition between these states often produces complicated dynamics (e.g., chaos, homoclinic bifurcations, blue sky catastrophes) more difficult to characterize [7, 8, 9, 10].

In this letter, we describe a novel mechanism for the transition from bursting to spiking activity observed in a realistic, biophysical model of a cerebellar Purkinje cell. We propose a reduction of this detailed model to study the transition and describe an intermediate state during which fast spiking activity is amplitude modulated by a slower rhythm. In this intermediate state we observe a new type of dynamics that follow the attracting and repelling branches of *limit cycles* in the fast subsystem. We compare these dynamics to traditional canard phenomena and propose that a new type of canard — a limit cycle canard — occurs in the reduced model and provides a potential explanation of the detailed model activity.

## Detailed and reduced models

The modeling and analysis were motivated by results observed in a detailed computational model of a cerebellar Purkinje cell [11, 12, 13]. The detailed model consists of 559 compartments, each with 12 types of ionic currents, resulting in over 6000 dynamical variables. We illustrate the results of a typical numerical simulation of this model in Figure 1. Between the quiescent intervals of bursts (Q), we observe rapid spiking activity modulated in amplitude (AM). This modulation becomes more complicated as time progresses until the activity reenters the quiescent burst phase. What dynamical and biophysical mechanisms produce this bursting activity interspersed with amplitude modulated spiking?

To answer this, we propose a reduced model of the de-



FIG. 1: Simulation results of the soma compartment voltage (black) from a detailed Purkinje cell model [13]. An injected current (gray) depolarizes the cell and produces rapid spiking modulated in amplitude (AM) followed by more complicated activity between the quiescent intervals (Q) of bursts. The horizontal and vertical scales (right) denote 50 ms and 50 mV, respectively.

tailed cerebellar Purkinje cell consisting of a single compartment with four ionic currents. The voltage and current dynamics follow:

$$\begin{aligned} \dot{V} = & -J - g_L(V + 70) - g_{Na}m_\infty[V]^3h(V - 50) \\ & - g_Kn^4(V + 95) - g_{Ca}c^2(V - 125) \\ & - g_M M(V + 95) \end{aligned} \quad (1a)$$

$$\dot{x} = \frac{x_\infty[V] - x}{\tau_x[V]}. \quad (1b)$$

Five currents affect the voltage in (1a): a leak current ( $g_L=2.0$ ), a transient inactivating sodium current ( $g_{Na}=125.0$ ), a delayed rectifier potassium current ( $g_K=10.0$ ), a high-threshold noninactivating calcium current ( $g_{Ca}=1.0$ ), and a muscarinic receptor suppressed potassium current (or M-current,  $g_M=0.75$ ). The dynamics of each gating variable follow (1b) with  $x$  replaced by  $h, n, c$ , or  $M$ . We implement the equilibrium function ( $x_\infty[V]$ ) and time constant ( $\tau_x[V]$ ) for each current from [14] and make the standard approximation of replacing the sodium activation variable with its equilibrium function ( $m_\infty[V]$ ). Of the five variables, the M-current evolves on a much slower time scale [15] and acts as the slow variable in this slow-fast system. In what follows, we increase the excitation of the reduced model neuron by increasing the magnitude of parameter  $J$  and compute numerical solutions and bifurcation diagrams for the system with XPPAUT and AUTO [16].

<sup>\*</sup>Department of Physiology & Pharmacology, SUNY Health Sciences Center, Brooklyn, NY, 11203, USA

<sup>†</sup>Department of Mathematics and Statistics, Boston University, Boston, MA, 02215, USA

### Simulation & bifurcation observations

We begin with a description of the voltage activity computed for decreasing values of the parameter  $J$  to illustrate the transition from bursting to rapid spiking. For  $J > -22.5$ , the dynamics approach a stable fixed point ( $V \approx -54$  mV for  $J = -22.5$ , not shown.) As we decrease  $J$  through  $-22.5$ , bursts of activity emerge (Figure 2, top). Within a burst the interval between, and amplitude of, the rapid spiking increase (from 1.6 ms to 2.0 ms, and 40 mV to 65 mV, respectively) after an initial transient. The interburst intervals (lasting approximately 200 ms) are much longer than the intervals between spikes. Decreasing  $J$  further we find that the burst duty cycle increases, but that the interval between burst onsets remains approximately constant. Near  $J = J_* = -32.93825$  the transition from bursting to rapid spiking begins and a new type of activity appears: bursts interspersed with amplitude modulated fast spiking activity (Figure 2, middle). We label the latter activity *torus spiking* to denote the two coexistent frequencies (i.e., the low frequency amplitude modulation of the high frequency spiking.) The new activity increases the interval between bursts by integer multiples of 120 ms, the period of one complete torus spike. In Figure 2 one torus spike separates the quiescent burst phases. We find (but do not show) that the number of torus spikes between bursts appears unpredictable; in simulations, we have observed between zero and 25 torus spikes between bursts. Reducing the parameter further to  $J = -32.94$  we find only torus spiking (and no bursting) activity. For  $J < -32.95$  only rapid spiking without amplitude modulation occurs and the transition from bursting to rapid spiking is complete.

What dynamical mechanisms govern the intermediate state between bursting and rapid spiking in the model? To address this, we examine the critical manifolds of the fast subsystem. In this slow-fast decomposition of (1), we fix  $J$ , treat the slow variable  $M$  in (1) as a parameter, and compute bifurcation diagrams numerically in AUTO as implemented in XPPAUT [16]. We then study the global dynamics of the full model on the critical manifold of the fast subsystem. For  $J = -23.0$  the dynamics exhibit well known behavior: rapid spiking begins at a fold of fixed points and ends at a fold of limit cycles (i.e., fold / fold cycle bursting [4]). But, as we decrease  $J$  towards  $J_*$ , we find novel activity develops as we now describe.

In Figure 3 we plot a bifurcation diagram (color) for the fast subsystem and simulation results for the full system (grayscale) with  $J = J_*$ . In the full system, rapid spiking begins when the M-current decreases past the fold of fixed points in the fast subsystem. The voltage then increases rapidly, and the full dynamics approach the attracting curve of limit cycles in the fast subsystem. With each spike, the slow M-current in the full system increases until the dynamics reach a fold of limit cycles in the fast subsystem. At this fold, we expect spiking to cease consistent with the fold / fold cycle bursting observed for  $J = -23.0$ . Instead we find that spiking con-

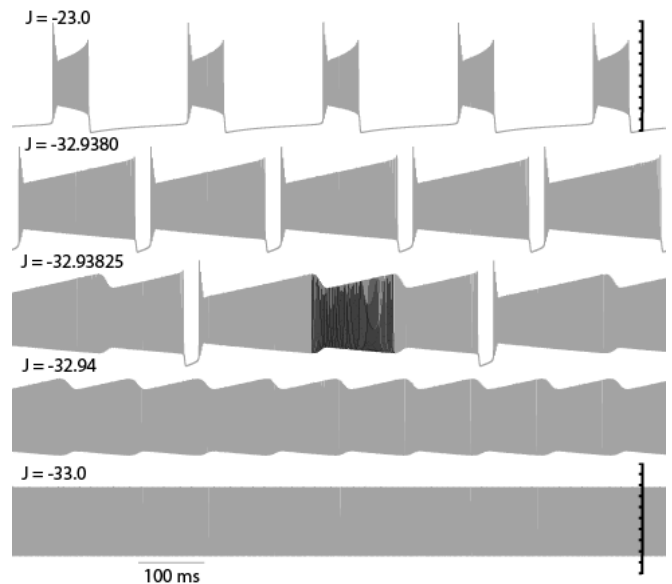


FIG. 2: The transition from bursting to torus spiking to rapid spiking in the reduced model as  $J$  decreases. We plot in gray the voltage activity of the neuron for five different values of  $J$ . In the middle trace ( $J = J_*$ ) we observe both bursting and torus spiking activity. We shade one cycle of a torus spike in black. Further reductions in  $J$  result in torus spiking and (unmodulated) spiking. The vertical bars in the top and bottom traces denote a 100 mV range, extending from -60 mV to 40 mV, with 10 mV between tick marks.

tinues as the dynamics of the full system follow the curve of limit cycles through the fold to the branch of *repelling* limit cycles. The M-current decreases, and the full dynamics follow temporarily the repelling branch of limit cycles until returning to the branch of attracting fixed points (light gray) or limit cycles (black). If the former, then the dynamics enter the quiescent phase of bursting and the M-current decreases. If the latter, then a torus spike occurs; rapid spiking continues and the dynamics again approach the fold of limit cycles as the M-current increases.

Decreasing  $J$  past  $J_*$  to  $-32.94$  eliminates bursting in the full model dynamics and results in torus spiking alone. During one cycle of a torus spike, the slow M-current in the full dynamics increases along the branch of attracting limit cycles, passes through the fold of limit cycles, and decreases along the branch of repelling limit cycles before returning to the branch of attracting limit cycles (Figure 4). As  $J$  decreases the extent of this slow modulation also decreases both in period (from approximately 0.11 s to 0.08 s) and in magnitude (the amplitude modulation of the rapid spiking decreases from approximately 16 mV to 0.5 mV). These reductions are suggested in Figure 4 and coincide with smaller excursions of the full dynamics from the fold point as  $J$  decreases. A torus bifurcation occurs in the full dynamics near  $J = -32.95$  and rapid spiking — without amplitude modulation — results. Decreasing

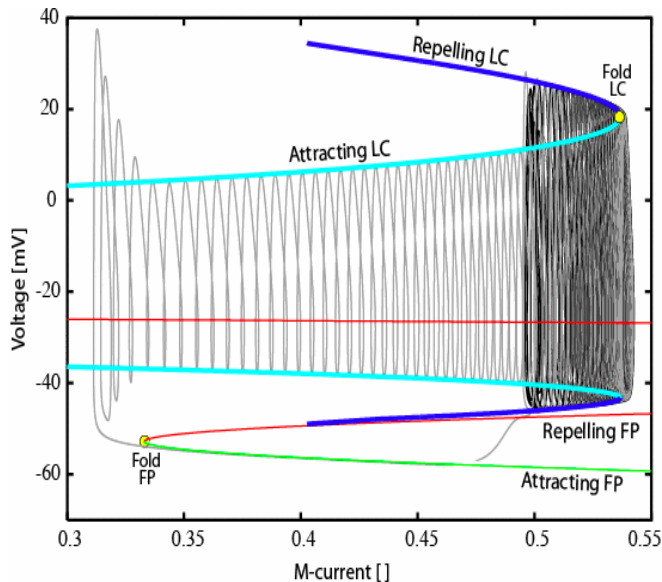


FIG. 3: Bifurcation diagram of the fast subsystem (color) and dynamics of the full system (grayscale) for  $J = J_*$ . In the fast subsystem, the attracting and repelling fixed points and limit cycles meet at folds (yellow circles) labeled Fold FP and Fold LC, respectively. The attracting limit cycles appear in a supercritical Hopf bifurcation (not shown) and the repelling limit cycles disappear in a homoclinic orbit bifurcation. At the fold of limit cycles (the slow) M-current changes direction and the complete dynamics follow the branch of repelling limit cycles temporarily until returning to the curve of attracting fixed points (burst in gray) or attracting limit cycles (torus spike in black).

$J$  further produces lower amplitude, faster oscillations that cease when  $J < -150$  and the supercritical Hopf bifurcation occurs at  $M > 1$ , outside the physiological range.

#### Comparison with canard formalism

We propose that the dynamics described above extend in new directions the classical canard phenomena observed in lower dimensional slow-fast systems. The prototypical canard example consists of two variables evolving on different time scales (e.g., the van der Pol equation.) For this two dimensional system, the critical manifold contains only curves of attracting and repelling fixed points. In the full system, the global dynamics follow the curve of attracting fixed points until reaching a fold in the critical manifold. At this fold — corresponding to a saddle node bifurcation of fixed points — the slow variable reverses direction and the full dynamics follow temporarily the curve of repelling fixed points of the fast subsystem, eventually returning to a stable branch of fixed points [17].

A related, but novel, phenomena appears to occur in the reduced, 5-dimensional model of the cerebellar Purkinje cell. The bifurcation diagram in Figure 3 corresponds to a projection of the 4-dimensional critical man-

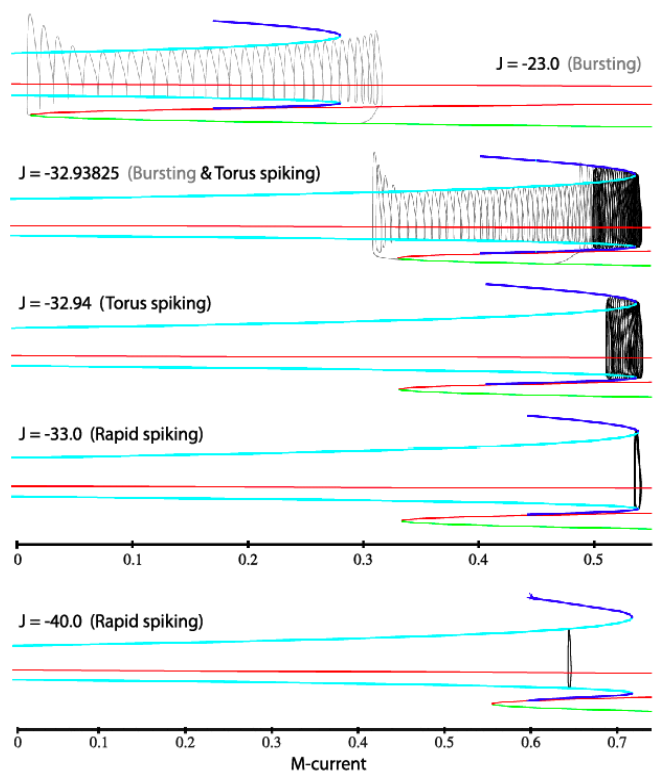


FIG. 4: Bifurcation diagrams of the fast subsystem (color) and dynamics of the full system (grayscale) for five different values of  $J$ . In all five figures, the range vertical axes are identical; the horizontal axes indicate the value of  $M$  and are expanded for the bottom figure. For  $J = -23$ , only fold / fold cycle bursting occurs (gray). At  $J = J_*$ , the dynamics follow temporarily the branch of repelling limit cycles, eventually returning to the branch of attracting fixed points (a burst, gray) or the branch of attracting limit cycle (a torus spike, black). Reducing  $J$  further results in torus spiking alone and rapid, unmodulated spiking.

ifold. During the active phase of the burst, the full model dynamics follow the curve of attracting limit cycles. Each (fast) cycle within the burst increases the (slow) M-current until the global dynamics reach a fold in the critical manifold. At this fold — corresponding to a saddle node bifurcation of *limit cycles* — the average dynamics of the slow variable reverse direction (i.e., the dynamics of the M-current averaged over individual spikes in the fast subsystem change sign from positive to negative.) The full dynamics then follow temporarily the curve of repelling *limit cycles*. Consistent with classical canard phenomena, the parameter value ( $J$ ) determines the length of time spent near the repelling branch and to which stable branch the dynamics return. What differs here is that the canard initiates not at a fold of fixed points, but at a fold of limit cycles. We therefore label this phenomena a limit cycle canard.

The limit cycle canard serves as an intermediary between the bursting and rapid spiking states. This is often the case with canards associated with dramatic

changes in dynamics resulting from small changes in a control parameter (e.g., a canard explosion from small amplitude limit cycles to large amplitude relaxation oscillations.) Here, the canard occurs in a small interval of the control parameter ( $J$  varies by approximately 0.012), but the transition from bursting to spiking does not appear instantaneous.

#### *Biophysical mechanisms*

The (slow) M-current and (fast) calcium current play complementary roles in the reduced model. During the active phase of a burst, the M-current acts to hyperpolarize the cell and discourage spiking, while the calcium current acts to depolarize the cell and promote spiking. When  $J > J_*$ , the hyperpolarization eventually wins, spiking stops, and the cell enters the quiescent phase of the burst. The M-current is essential to this bursting activity [18]. For  $J < J_*$ , the depolarizing effect of the calcium current prevents the runaway hyperpolarization due to the M-current. The quiescent phase of the bursts no longer occurs and we find instead only slow modulation of the fast spiking activity. Decreasing  $J$  further reduces the the M-current dynamics and produces unmodulated fast spiking activity. We note that, in the reduced model, blocking either the M or calcium current during amplitude modulated rapid spiking produces unmodulated rapid spiking. These predictions were confirmed in the detailed model.

#### *Conclusions*

In this letter we describe a novel mechanism that occurs during the transition from bursting to rapid spiking activity: limit cycle canards. We identified this activity in a physiologically realistic computational model of a cerebellar Purkinje cell that motivated the simplified mathematical model. By studying the slow-fast dynamics of the reduced system, we developed a better understand-

ing of the physiological mechanisms (the M-current and calcium current) and dynamical mechanisms (the limit cycle canard) that could produce the activity observed in the detailed model.

Canards have been observed in other mathematical models of neural systems [19, 20, 21, 22]. However, in all of these systems, the canards occur along branches of attracting and repelling fixed points. The dynamics presented here are unique in that the canards occur along branches of attracting and repelling limit cycles. In addition, these results were not limited to the reduced model; similar dynamics were also observed in a detailed biophysical model. Moreover, the slow modulation of the fast spiking activity appears to occur *in vitro* (see Figures 7A and 8A of [23]). Additional recordings of cerebellar Purkinje cells could test experimentally the existence of limit cycle canards and the role of the M-current in these dynamics.

Our analysis focused on a computational, slow-fast decomposition of (1). Although useful, this decomposition appears inadequate; we note in particular that small changes in the middle three bifurcation diagrams of Figure 4 coincide with large changes in the full dynamics (namely, the transition from bursting to torus spiking to rapid spiking). A better understanding of these dynamics will require a more systematic singular perturbation treatment [24, 25] and perhaps a reduction from five to fewer dimensions [26]. We note that the transition from bursting to spiking exhibits a mixed mode oscillation pattern (with bursts acting as the large amplitude oscillations and torus spikes as the small amplitude oscillations) [27]. The system may therefore benefit from this type of analysis as well.

The authors thank Tasso J. Kaper and Horacio G. Rotstein for useful suggestions and discussions. NJK is supported by NSF DMS-0727670. MAK is supported by an NSF RTG Grant.

- 
- [1] J. Lisman, *Trends Neurosci.* **20**, 38 (1997).  
 [2] E. Izhikevich et al., *Trends Neurosci.* **26**, 161 (2003).  
 [3] J. Rinzel, in *Lecture notes in biomathematics*, edited by E. Teramoto and M. Yamaguti (Springer-Verlag, 1987), vol. 71, pp. 267–281.  
 [4] E. Izhikevich, *Int. J. Bifurcat. Chaos* **10**, 1171 (2000).  
 [5] A. L. Hodgkin and A. F. Huxley, *J Physiol (Lond)* **117**, 500 (1952).  
 [6] E. Izhikevich, *Dynamical Systems in Neuroscience* (MIT Press, 2007).  
 [7] D. Terman, *J. Nonlinear Sci* **2**, 135 (1992).  
 [8] X. Wang, *Physica D* **62**, 263 (1993).  
 [9] V. Belykh et al., *Eur Phys J E* **3**, 205 (2000).  
 [10] A. Shilnikov and G. Cymbalyuk, *Phys Rev Lett* **94**, 048101 (2005).  
 [11] T. Miyasho et al., *Brain Res* **891**, 106 (2001).  
 [12] S. J. Middleton et al., *Neuron* (in press).  
 [13] R. D. Traub et al., in *Society for Neuroscience Annual Convention* (2008), 793.10/L23.  
 [14] R. D. Traub et al., *J Neurophysiol* **89**, 909 (2003).  
 [15] J. V. Halliwell and P. R. Adams, *Brain Res* **250**, 71 (1982).  
 [16] B. Ermentrout, *Simulating, Analyzing, and Animating Dynamical System* (SIAM, 2002).  
 [17] M. Diener, *Math Intell* **6**, 38 (1984).  
 [18] A. K. Roopun et al., *Proc Natl Acad Sci USA* **103**, 15646 (2006).  
 [19] J. Guckenheimer, K. Hoffman, and W. Weckesser, *Int. J. Bifurcat. Chaos* **10**, 2669 (2000).  
 [20] H. G. Rotstein et al., *SIAM J Appl Math* **63**, 1998 (2003).  
 [21] J. Moehlis, *J. Math. Biol.* **52**, 141 (2006).  
 [22] J. Rubin and M. Wechselberger, *Biol. Cyber.* **97**, 5 (2007).  
 [23] R. Llinás and M. Sugimori, *J Physiol (Lond)* **305**, 171 (1980).  
 [24] A. Milik and P. Szmolyan, in *Multiple-time-scale dynamical systems*, edited by C. K. R. T. Jones and A. Khibnik (Springer-Verlag, 2001), vol. 122, pp. 117–140.

- [25] P. Szmolyan and M. Wechselberger, *J. Differ. Equations* **177**, 419 (2001).
- [26] G. S. Medvedev, *Phys Rev Lett* **97**, 048102 (2006).
- [27] M. Brons, M. Krupa, and M. Wechselberger, *Fields Institute Communications* **49**, 39 (2006).